Journal of the Optical Society of Korea, Vol. 9, No. 4, December 2005, pp. 151-156

A Spatial-domain Fourier Transform Infrared Spectrometer: Application for Analyte Measurement in Cell Culture Media

Byungjo Jung*

Department of Biomedical Engineering, Yonsei University, Wonju 220-710, Korea

(Received September 22, 2005 : revised November 15, 2005)

A spatial-domain Fourier Transform (FT) infrared (IR) spectrometer coupled with a PtSi Schottky-barrier IR detector plane was developed in the spectral range of 2.0-2.5 μm for noninvasive measurement of analyte concentrations in cell culture media during cell culture processing. A key optical component of the spectrometer is a Savart plate which is a birefringent polarizer generating coherent two rays for interfering. The spectral resolution of the spectrometer was determined as 71 cm^{-1} (~0.05 μm at 2.5 μm). Clear IR fringe patterns were imaged on the IR detector plane. The feasibility of the spectrometer for our application was investigated by measuring absorbance spectra of glucose and fetal bovine serum (FBS) which are important compounds in cell culture media. Experiment results show that the spectral quality of glucose and FBS was comparable with the standard spectra acquired with a commercial FT-IR spectrometer, presenting the feasibility of the spectrometer to perform analyte measurement in cell culture media.

OCIS codes : 170.0170, 300.0300, 300.6190, 300.6340

I. INTRODUCTION

Noninvasive monitoring of analyte concentrations in cell culture media is important in biological and biotechnological experiments. Near infrared (NIR) absorption spectroscopy was proposed as a possible noninvasive optical method for monitoring of analyte concentrations in cell culture media during cell culture process [1]. The absorbance spectrum of cell culture media can be acquired with a FT-IR spectrometer which provides a high spectral resolution measurement for a wide variety of radiations and offers distinct throughput (Jaquinot) and multiplex (Fellget) advantages over dispersive spectrometers [2]. However, the bench-top FT-IR spectrometer has drawbacks in the application for cell culture process monitoring, namely the high-cost due to the requirement of high-quality mirror-scanning mechanism, the high sensitivity to external perturbation due to the moving mirror, the requirement of long measurement time to get a spectrum having high signal-to-noise ratio (SNR), and the limited temporal resolution due to the maximum mechanical scanning rate. Part of those drawbacks can be potentially overcome by a spatial-domain FT-IR spectrometer in which, unlike conventional FT-IR spectrometer, the interferogram is acquired in the spatial-domain rather than the time domain.

The spatial-domain FT-IR spectrometer has been studied over the past several years [3-24]. It consists of a two-beam interferometer and a multi-channel detector sensor (a linear array detector or a 2-D focal plane array) for recording the interferogram. commonly used types of interferometers include the triangular common-path interferometer [3-8], the Michelson interferometer with a tilted mirror [9, 10], and the polarization interferometer utilizing a Savart plate [11, 12] or a Wollaston prism [7, 11, 13-20]. Most of the spectrometers are in the research stage and as far as I know, there is no commercially available one.

The advantages of this type of spectrometer compared to the conventional FT-IR spectrometer are attributed to the potential for a compact optical setup at a low cost, the less sensitivity over external perturbation, the simple and durable optical setup without moving parts. With those advantages, the spatial-domain FT-IR spectrometer has a potential as a useful noninvasive optical tool for measurement of analyte concentrations in culture media during cell culture processing.

A spatial-domain FT-IR spectrometer based on a Savart plate was built in the spectral range of 2.0 - 2.5 μm (5000-4000 cm^{-1}). In addition, a temperature-controlled cell holder built in laboratory was integrated into the spectrometer system to maintain the temperature of the sample solution at a constant level. Using the spectrometer system, this study, as an initial study for our application,

was focused on the investigation of whether or not it can be utilized to acquire absorbance spectra of analytes in cell culture media. The feasibility was investigated by measuring absorbance spectra of glucose and fetal bovine serum (FBS) which are important chemical and biological compounds in cell culture media and comparing those spectra with standard absorbance spectra acquired with a commercial FT-IR spectrometer.

II. THEORY

1. Absorbance spectrum

The NIR absorbance spectrum contains molecular structural information and physical properties. According to Beer's law, the absorbance of the sample can be used to determine the sample concentration. Beer's law states that the absorbance of a sample is directly proportional to its concentration in an aqueous solution [25]. The following is the formula for Beer's law

$$A = -\ln(I_i/I_o) = \varepsilon LC \quad (1)$$

where A is the absorbance of a medium, L is the optical pathlength, C is the medium concentration, ε is the molar absorptivity, I_i is the intensity of the incident light, and I_o is the intensity of the transmitted light. The absorbance spectrum (AS) of a sample can be calculated using the equation 2 in which A_{sample} and $A_{reference}$ are a single-beam spectrum of sample solution and reference solution, respectively.

$$\text{AS} = \log(\text{Areference} / \text{Asample}) \quad (2)$$

2. Principles of Savart plate

A key optical component in the spatial-domain FT-IR spectrometer is a Savart plate [7, 14-16, 20, 25] which produces two linearly polarized rays, ordinary (o) and extraordinary (e) rays. It is composed of a combination of two identical crystal plates that are cut at 45° to the optical axis of the system with their principle section crossed. The lateral displacements produced by each of the two component plates are equal and in perpendicular directions. The total relative displacement will thus be $\sqrt{2}$ times the displacement produced by each plate. For a Savart plate of total thickness $2t$ the lateral displacement (S) [26] of the two rays is

$$S = \sqrt{2}\frac{n_o^2 - n_e^2}{n_o^2 + n_e^2}t \quad (3)$$

where n_e and n_o are the index of refraction value for the e- and o-ray, respectively, and t is the thickness of the crystal plate. This gives a value $8\times10^{-3}t$ for quartz and $0.15t$ for calcite.

3. Spectral resolution

X position (raw pixel position) on the detector plane has to be calibrated to express the spectrum as a function of wavenumber (a reciprocal of wavelength). In order to compute the spectrum as a function of spatial frequency, maximum Nyquist frequency (δ_{max}) in wavenumber (cm^{-1}) has to be calculated as follows [4, 11, 22]:

$$\delta_{max} = (N/2)*\delta \quad (4)$$

Where N is the number of raw pixels on the detector plane illuminated by fringe pattern and δ is the spectral resolution in wavenumber. If the fringe pattern is magnified on the detector plane, a magnification factor has to be then considered in the equation (4). The theoretical resolution at the full width at half maximum (FWHM) is inversely proportional to the optical path difference of two rays. The optical path difference (Γ) between two rays at the X position on the detector plane is given by

$$\Gamma = SX/f = SND/f. \quad (5)$$

Where S is the lateral distance of two split rays, f is focal length of imaging lens, and X is an arbitrary spatial location on the detector plane that is equal to the production of the number of pixels (N) and pixel width (D) in the raw pixels. Using Rayleigh criterion with triangular apodization, the spectral resolution can be written as

$$\delta = 1/\Gamma = f/(SND) \quad (6)$$

III. EXPERIMENTAL

1. Instrumentation design

A diagram and picture of the spatial-domain FT-IR spectrometer based on a custom ordered Savart plate are shown in Fig. 1 (a) and (b), respectively. A 100W tungsten-halogen lamp (Oriel Instruments, Stratford, CA) was employed as a light source and a 2.0 μm cut-on long-wave pass interference filter (Oriel Instruments, Stratford, CA) was placed across the incident ray. In order that the o- and e-rays produced by the Savart plate (Halbo Optics, Chelmsford, UK) were coherent with each other, a Glan-Taylor polarizer (P1) (Melles Griot, Irvine, CA) was placed across the incident ray so that only a single component of the natural light was transmitted on to the Savart plate. In order to equally orthogonally distribute the amplitude of the incident ray, the transmission direction of this polarizer (P1) was set at 45° to the privileged directions of the Savart plate. The o- and e-rays produced by the Savart plate vibrate in orthogonal direction. In order to interfere each other, their directions of vibration should be

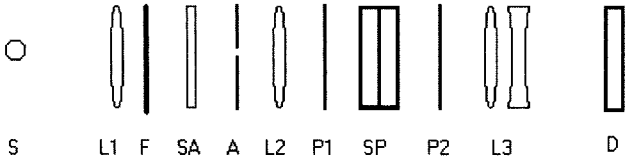

(a)

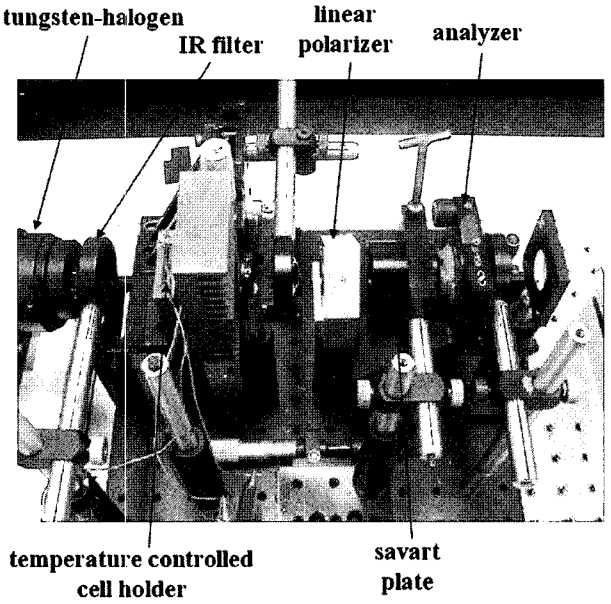

(b)

FIG. 1. (a) A schematic diagram and (b) picture of the spatial-domain FT-IR spectrometer. The system consists of S, a tungsten-halogen lamp; L1 (f = 100 mm) and L2 (f = 25 mm), focusing lens; F, an IR filter; A, an aperture; P1 and P2, polarizer; SP, a Savart plate; L3 (f = 25 mm, f = -25 mm), a lens combination for interference and imaging; SA, a temperature controlled cell holder; D, an IR detector.

set parallel to each other. This was achieved by means of another Glan-Taylor polarizer (P2) (Melles Griot, Irvine, CA) called an analyzer. The transmission direction of the analyzer was set at 45° to the two orthogonal vibrations in order for the two interfering beams to become equal in the amplitude. Finally, an imaging lens combination was used to fit the fringe pattern on the detector plane (D). An IR-M700 PtSi Schottky-barrier IR detector (Mitsubishi Electronics, Cypress, CA) with 801 by 512 pixel elements was utilized to image the IR fringe pattern.

2. Procedure for absorbance spectrum computation

The absorbance spectrum of a sample was acquired from the spatial-domain FT-IR spectrometer. First, the polarizer (P1) was rotated 0° and 90° to the analyzer (P2) in order to acquire the in-phase and anti-phase fringe patterns. This rotation creates 180° phase difference between in-phase and anti-phase fringe. Second, the in-phase and anti-phase 1-D interferograms were calculated by averaging column pixels from their own fringe image. The anti-phase interferogram was subtracted from the in-phase interferogram so that the background distribution caused by noninterference light can be removed and the interferogram signal becomes twice as large. The average value of the subtracted interferogram was also subtracted from the interferogram in order to remove DC offset of the interferogram. Third, a triangular apodization was applied to the interferogram to reduce the side-lobes in the spectrum and make a periodic signal before calculating the spectrum. Finally, a single-beam spectrum was calculated by applying the Fast Fourier Transform (FFT) to the triangularly apodized interferogram. The single-beam spectra of the reference and sample solution were acquired with the procedures described above and finally, a sample absorbance spectrum was calculated by equation 2.

3. Reagents and procedure

A glucose solution (sample solution) was prepared by dissolving crystalline dextrose (EM Science, Gibbstown, NJ) in the phosphate buffer solution (reference solution) of PH 7.0 and a RPMI 1640 cell culture media including 10 % FBS was also prepared at room temperature. The solutions were placed in a rectangular Infrasil quartz cell (Starna, Atascadero, CA) with optical pathlength of 1 mm. The sample cell was placed in a temperature-controlled cell holder [27] made in the laboratory in the which temperature of the sample solution was maintained at desired value. A T-type thermocouple wire (Omega, Stamford, CT) was submerged directly into the sample cell and the temperature was monitored with a digital thermometer (Omega, Stamford, CT).

IV. RESULTS AND DISSCUSSION

The lateral displacement of the two rays is a function of the thickness of the Savart plate when refractive indices of the birefringent material were known. Each crystal of the custom-ordered Savart plate has the same thickness of 15 mm. Therefore, the lateral displacement (D) was found to be 2.3141 mm with the refractive indices of calcite in which n_o = 1.658 and n_e = 1.486.

In order to compute the spectral resolution given by equation 6, maximum optical path difference was first calculated. The IR detector was adjusted for the center burst of the interferogram to be located at the 400th raw pixel on the IR detector plane. This pixel position was used as an origin to calculate maximum optical path difference. In the spectrometer, L2 was 125 mm, S 2.3141 mm, N 400, and D 17 μm. By applying triangular apodization to the interferogram, the resolution was

determined as 71 cm^{-1} (0.05 μm at 2.5 μm). According to the equation 6, the most straightforward method to enhance spectral resolution is to use an IR detector plane having a larger number of pixels. However, as far as I know, there is no commercially available IR detector array or plane having more than 800 raw pixels in the spectral range of interested. Alternatively, the spectral resolution can be improved as much as two times by using one-side interferogram instead of a double-side interferogram. The spectral resolution can also be optically enhanced by using thicker Savart plate to increase lateral displacement of two rays or by using the lens, L2 with shorter focal length. In addition, there are several mathematical methods to improve spectral resolution [28, 29]. We are studying those methods to obtain better spectral resolution in the spectrometer.

The IR fringe pattern of a tungsten-halogen lamp was acquired in the spectral range of 2.0 - 2.5 μm and presented in Fig. 2a. The 1-D interferogram of the in-phase (solid-line) and anti-phase (dotted-line) fringe was computed, and the central part of the interferogram was presented in Fig. 2b. The results show the capability of the spectrometer of detecting the IR fringe pattern and the feasibility of acquiring the IR spectrum.

The standard glucose absorbance spectra at various resolutions were acquired with a commercial bench-top FT-IR spectrometer (Mattson, Madison, WI). Fig. 3(a) depicts the standard absorbance spectra at the resolutions of 4 cm^{-1}(0.003 μm at 2.5 μm), 64 cm^{-1} (0.04 μm at 2.5 μm), and 128 cm^{-1} (0.078 μm at 2.5 μm) when being read

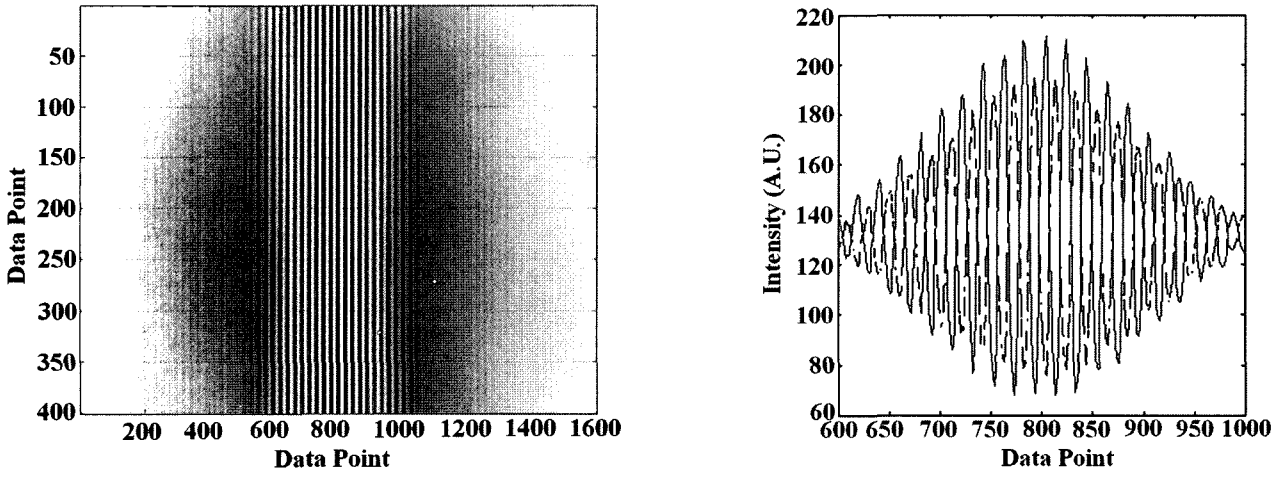

(a) (b)

FIG. 2. (a) An IR fringe image of a tungsten-halogen lamp and (b) processed in-phase (solid-line) and anti-phase (dotted-line) interferogram.

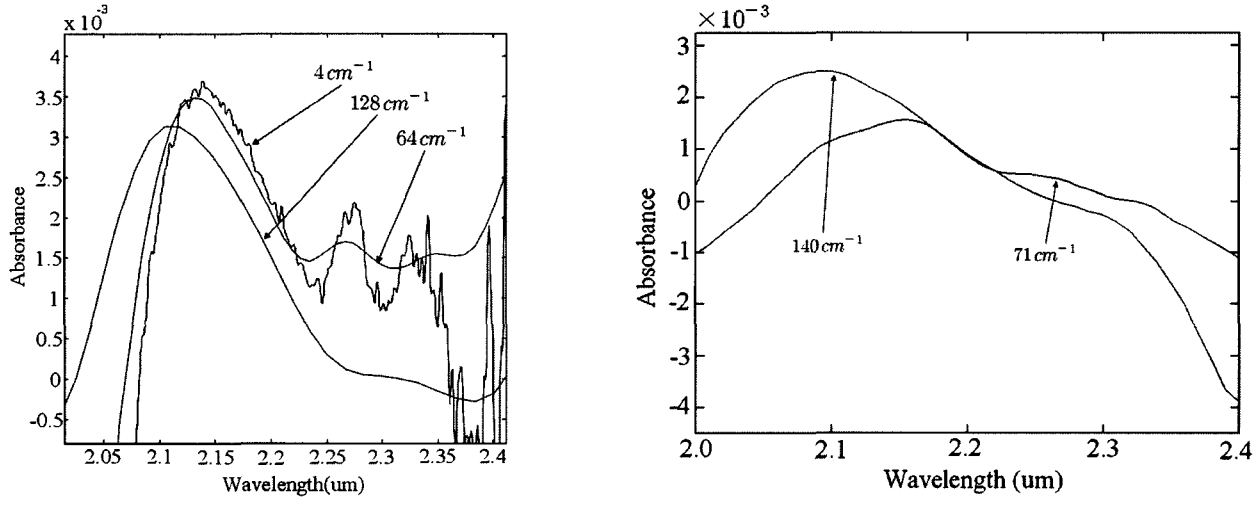

(a) (b)

FIG. 3. (a) Standard glucose absorbance spectra collected with a commercial FT-IR spectrometer and (b) glucose absorbance spectra collected at the resolution of 71 cm^{-1} and 140 cm^{-1} with the spatial-domain FT-IR spectrometer. Their won resolution was marked in the graph.

from bottom to top at 2.27 μm. As seen in the figure, increasing resolution resulted in decreasing SNR. Therefore, one needs to trade off between the resolution and the SNR of spectrum. For comparison, glucose absorbance spectra were acquired at two different resolutions of 71 cm^{-1} (0.05 μm at 2.5 μm) and 140 cm^{-1} (0.1 μm at 2.5 μm) with the spatial-domain FT-IR spectrometer (Fig. 3b). In Fig. 3b, the fringe pattern at the resolution of 140 cm^{-1} was magnified about two times and all pixels on the IR detector were used to maintain the same data point. When compared to the standard spectra, these two spectra show similar absorbance peaks and spectral shape, presenting the feasibility of the spatial-domain FT-IR spectrometer for glucose measurement.

The absorbance spectra of FSB have two strong absorbance peaks at 2.18 μm (4587 cm^{-1}) and 2.28 μm (4386 cm^{-1}). Three standard FBS absorbance spectra were collected and presented in Fig. 4a. The resolutions of the spectra were 128 cm^{-1}, 4 cm^{-1}, 64 cm^{-1} when being read from top to bottom at 2.25 μm. For further examination of the feasibility of the spatial-domain FT-IR spectrometer, two FBS absorbance spectra at the resolution of 71 cm^{-1} and 140 cm^{-1} were also collected and presented in Fig. 4b in which the spectra at the resolution of 71 cm^{-1} and 140 cm^{-1} were presented from top to bottom at 2.18 μm, respectively. As illustrated in the figure, two absorbance peaks were clearly resolved.

Since the spatial-domain FT-IR spectrometer has not been optimized in terms of throughput and spectral resolution, the spectra shown in Fig. 3 and 4 are not sufficient in quality when compared with standard ones. In the current system, a UV grade fused silica lens has a high attenuation at 2.25 μm which is close to the glucose absorption peak. By replacing by an IR grade lens, throughput of the system might be increased.

V. CONCLUSIONS

The spatial-domain FT-IR spectrometer without moving parts was developed to replace the conventional FT-IR spectrometer during cell culture process monitoring. The spatial-domain FT-IR spectrometer had a maximum resolution of 71 cm^{-1}. The spectral resolution can be further improved by using an imaging lens having a shorter focal length, applying mathematical methods, and adjusting detector plane location to detect one-side interferogram.

Glucose and FBS absorbance spectra were measured and compared with standard spectra. In both cases, spectral shape and absorbance peaks were comparable with standard ones. However, the glucose absorbance peaks were not clear at low concentrations. The quality of the spectrum can be improved by using the IR optics and the mathematical method for post signal processing. Now, we are trying to detect the absorbance spectrum at low glucose concentration and to enhance spectral resolution. Finally, application of the spatial-domain FT-IR spectrometer is not restricted to the IR spectral range. The use of the current spatial-domain FT-IR spectrometer depends on the spectral response of the detector array or plane and optics.

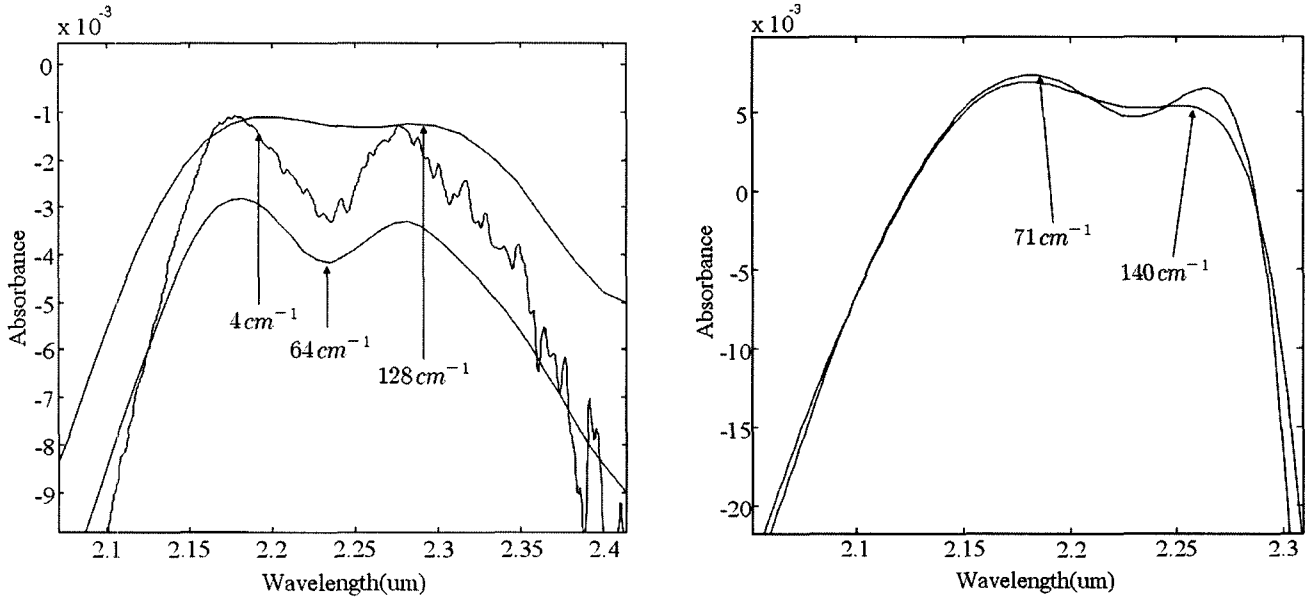

FIG. 4. (a) Standard absorbance spectra of 10% FBS and (b) FBS absorbance spectra collected at the resolution of 71 cm^{-1} and 140 cm^{-1} with the spatial-domain FT-IR spectrometer. Their won resolution was marked in the graph.

ACKNOWLEDGEMENT

This work was supported by Yonsei University Research Fund of 2005.

*Corresponding Author: bjung@dragon.yonsei.ac.kr

REFERENCES

[1] B. Jung, S. Lee, I. Yang, T. Good, and G. Cote', "Automated on-line noninvasive optical glucose monitoring in a cell culture system," *Appl. Spectrosc.*, vol 56, pp. 51-57, 2002.

[2] V. Saptari, "*Fourier-Transform spectroscopy Instrumentation Engineering*," *A.R. Weeks de.*, (SPIE Press, Washington, 2003) pp. 4-9.

[3] M. Hashimoto and H. Hamaguchi, "Construction of a multichannel Fourier Transform Infrared spectrometer for single-event time-resolved spectroscopy," *Appl. Spectrosc.*, vol. 50, pp. 1030-1033, 1996.

[4] T. Okamoto, S. Kawata, and S. Minami, "Optical method for resolution enhancement in photodiode array Fourier Transform spectroscopy," *Appl. Opt.*, vol. 24, pp. 4221-4225, 1985.

[5] J. Zhao and R. L. Mccreery, "Multichannel Fourier Transform Raman spectroscopy: combining the advantages of CCDs with interferometry," *Appl. Spectrosc.*, vol. 50, pp. 1209-1214, 1996.

[6] M. P. Dierking and M. A. Karim, "Solid-block stationary Fourier-Transform spectrometer," *Appl. Opt.*, vol. 35, pp. 84-89, 1996.

[7] S. Minami, "Fourier Transform spectroscopy using image sensors," *Mikrochimica Acta*, vol. 3, pp. 309-324, 1987.

[8] J. V. Weedler and M. B. Denton, "Spatially encoded Fourier Transform spectroscopy in the ultraviolet to Near-Infrared," *Appl. Spectrosc*, vol. 43, pp. 1378-1384, 1989.

[9] H. Aryamanya-Mugisha and R. R. Williams, "A Fourier Transform diode array spectrometer for the UV, visible, and Near-IR," *Appl. Spectrosc*, vol. 39, pp. 693-696, 1985.

[10] M. L. Junttila, J. Kauppinen, and E. Ikonen, "Performance limits of stationary Fourier spectrometers," *J. Opt. Soc. Am.*, vol. 8, pp. 1457-1462, 1991.

[11] N. Ebizuka, M Wakaki, Y Kobayashi, and S. Sato, "Development of a multichannel Fourier spectrometer," *Appl. Opt.*, vol. 34, pp. 7899-7906, 1995.

[12] M. Hashimoto and S. Kawata, "Multichannel Fourier-Transform infrared spectrometer," *Appl. Opt.*, vol. 31, pp. 6096-6101, 1992.

[13] M. J. Padgett and A. R. Harvey, "A static Fourier-Transform spectrometer based on Wollaston prisms," *Rev. Sci. Instrum.*, vol. 66, pp. 2807-2811, 1995.

[14] J. Courtial, B. A. Patterson, A. R. Harvey, W. Sibbett, and M. J. Padgett, "Design of a static Fourier-transform spectrometer with increased field of view," *Appl. Opt.*, vol. 35, pp. 6698-6702, 1996.

[15] X. Q. Jiang, J. Kemp, Y. N. Nign, A. W. Palmer, and K. T. V. Grattan, "High-accuracy wavelength-change measurement system based on a Wollaston interferometer incorporating a self-referencing scheme," *Appl. Opt.*, vol. 36, pp. 4907-4912, 1997.

[16] B. A. Patterson, M. Antoni, J. Courtial, A. J. Duncan, W. Sibbett, and M. J.Padgett, "An ultra-compact static Fourier-Transform spectrometer based on a single birefringent component," *Opt. Commun.*, vol. 130, pp. 1-6, 1996.

[17] J. Courtial, B. A. Patterson, W. Hirst, A. R. Harvey, A. J. Duncan, W. Sibbett, and M. J. Padgett, "Static Fourier-Transform ultraviolet spectrometer for gas detection," *Appl. Opt.*, vol. 36, pp. 2813-2817, 1997.

[18] M. J. Padgett, A. R. Harvey, A. J. Duncan, and W. Sibbett, "Single-pulse, Fourier-Transform spectrometer having no moving parts," *Appl. Opt.*, vol. 33, pp. 6035-6040, 1994.

[19] T. H. Barnes, "Photodiode array Fourier Transform spectrometer with improved dynamic range," *Appl. Opt.*, vol. 24, pp. 3702-3706, 1985.

[20] T. Okamoto, S. Kawata, and S. Minami, "Photodiode array Fourier Transform spectrometer based on a birefringent interferometer," *Appl. Spectrosc*, vol. 40, pp. 691-695, 1986.

[21] W. Baird and N. S. Nogar, "Compact, self-contained optical spectrometer", *Appl. Spectrosc.*, vol. 49, pp. 1699-1740, 1995.

[22] S. Takahashi, J. S. Ahn, S. Asaka, and T. Kitagawa, "Multichannel Fourier Transform spectroscopy using two-dimensional detection of the interferogram and its application to Raman spectroscopy," *Appl. Spectrosc.*, vol. 47, pp. 863-868, 1993.

[23] M. L. Junttila, "Stationary Fourier-Transform spectrometer," *Appl. Opt.*, vol. 31, pp. 4106-4112, 1992.

[24] T. H. Barnes, T. Eiju, and K. Matsuda, "Heterodyned photodiode array Fourier Transform spectrometer," *Appl. Opt.*, vol. 25, pp. 1864-1866, 1986.

[25] D. A. Skoog, F. J. Holler, and T. A. Nieman, "*Principles of Instrumental Analysis*," (Thomson Learning, Stamford, 1998) pp. 189-140.

[26] M. Francon and S. Mallick, "*Polarization Interferometers: Application in Microscopy and Macroscopy*," (John Wiley & Sons, New York, 1971) pp. 19-25.

[27] B. Jung, "*Effects of temperature on Near-Infrared spectroscopic measurement of glucose*," (Texas A&M University, College Station, 1998) pp 10-11.

[28] S. Kawata, K. Minami, and S. Minami, "Superresolution of Fourier Transform spectroscopy data by the maximum entropy method," *Appl. Opt.*, vol. 22, pp. 3593-3598, 1983.

[29] K. Minami, S. Kawata, and S. Minami, "Supperresolution of Fourier Transform spectra by autoregressive model fitting with singular value decomposition," *Appl. Opt.*, vol. 24, pp. 162-167, 1985.